



*Undersea Research Centre*

*Centre de Recherche Sous-Marine*

Comparison of a time domain  
spectral collocation method  
and the time-evolution  
backscatter model  
BORIS

*O. Bergem  
T. Jenserud*

Comparison of a time domain  
spectral collocation method  
and the time-evolution  
backscatter model BORIS

O. Bergem, T. Jenserud

---

The content of this document pertains to  
work performed under Project 033-2 of  
the SACLANTCEN Programme of Work.  
The document has been approved for  
release by The Director, SACLANTCEN.



Jan L. Spoelstra  
Director

intentionally blank page

Comparison of a time domain spectral collocation method and the time-evolution backscatter model BORIS

O. Bergem, T. Jenserud

**Executive Summary:**

Reverberation from the seabed is one of the principal factors degrading the capability of minehunting sonars to detect ground mines. The acoustic scattering processes giving rise to this reverberation are complex phenomena for which several models are available. However, the majority of the existing models were developed for frequencies lower than those of interest for minehunting applications.

Accurate seabed acoustic scattering models may also be used for remote sensing using inversion techniques; if the acoustic response of the seabed is measured, its properties can be determined. Inversion techniques require many iterations for success and consequently model speed is an important factor. SACLANTCEN has recently developed a new model, Bottom Response from Inhomogeneities and Surface (BORIS), which emphasizes the acoustic scattering contributions of the seafloor roughness and the sediment inhomogeneities in the first metre or so of the seabed. The BORIS model is largely analytical and therefore the calculation speed is fast. BORIS has been validated using data recorded at sea but it is difficult to measure accurately the seafloor parameters for the recorded data.

A alternative model to BORIS has been developed by Forsvarets Forskningsinstitutt (NDRE); this model is entirely numerical which should theoretically provide more accurate answers than BORIS does but at the expense of much longer calculation times. Therefore, a comparison with this reference model has been carried out with the aim of a further validation of the BORIS model.

This report describes the comparison between the two models with specific reference to the different approximations, model limitations and levels of confidence. The comparison has been carried out at medium frequency (6 kHz) so that the NDRE reference model could be run on a standard workstation, but the validation of the SACLANTCEN BORIS model is applicable also to higher frequencies. The results from the two models are sufficiently similar to increase confidence in the analytical approach adopted in BORIS.

intentionally blank page

**Comparison of a time domain spectral collocation method and the  
time-evolution backscatter model BORIS**

O. Bergem, T. Jensenrud

**Abstract:** A model based on the time-domain spectral collocation method has been implemented at Forsvarets Forskningsinstitut (NDRE). The model can predict the time-series response from a seafloor defined by two two-dimensional matrices of compressional sound speed and density. At SACLANTCEN, a model named BORIS (**B**ottom **R**esponse from **I**nhomogeneities and **S**urface) based on the time-evolution approach has recently been developed. Both models are briefly described, and the implication of the different assumptions and limitations in both models are discussed. Five test-cases have been defined in order to study and compare the responses. The test-cases range from a flat, homogeneous bottom to a bottom containing both roughness and volume inhomogeneities. The comparisons show that the two models give similar results both from the surface and from the volume inhomogeneities. The absolute levels of the signals from the spectral collocation model are generally slightly higher than the levels from the BORIS model. This is believed to be due to the two-dimensional limitations in the spectral model.

**Keywords:** ◦ seafloor backscatter ◦ BORIS model ◦ spectral collocation method ◦ model comparison

## Contents

1	Introduction . . . . .	1
2	BORIS model . . . . .	2
3	Spectral collocation model . . . . .	5
3.1	Numerical methods for rough surface scattering problems . . . . .	5
3.2	Physical model and numerical implementation . . . . .	6
4	Differences between the models . . . . .	10
4.1	Two versus three dimensions . . . . .	10
4.2	Single versus multiple scattering . . . . .	11
4.3	Inhomogeneity description . . . . .	11
4.4	Attenuation . . . . .	12
4.5	Bottom discretization . . . . .	12
5	Simulation setup . . . . .	13
5.1	Pulse and geometry . . . . .	13
6	Model comparison results . . . . .	16
6.1	Case 1: Flat and homogeneous bottom . . . . .	16
6.2	Case 2: Rough and homogeneous bottom . . . . .	17
6.3	Case 3: Flat and inhomogeneous bottom without impedance contrast . . . . .	17
6.4	Case 4: Flat and inhomogeneous bottom . . . . .	18
6.5	Case 5: Rough and inhomogeneous bottom . . . . .	18
7	Summary . . . . .	19
7.1	Future work . . . . .	19
	References . . . . .	20
	Annex A - Figures from test runs . . . . .	22

## List of Figures

---

1	Simplified box diagram of the model. . . . .	4
2	Model geometry for the scattering problem. . . . .	7
3	The time-series of the pulse . . . . .	14
4	The beam pattern of the source . . . . .	14
5	The sound velocity profile, case 1 . . . . .	23
6	The sound velocity profile, case 2 . . . . .	23
7	The sound velocity profile, case 3 . . . . .	23
8	The sound velocity profile, case 4 . . . . .	24
9	The sound velocity profile, case 5 . . . . .	24
10	Result from BORIS, case 1 . . . . .	25
11	Result from spectral collocation model, case 1 . . . . .	25
12	Result from BORIS, case 2-5 . . . . .	26
13	Result from spectral collocation model, case 2-5 . . . . .	26
14	The figure show a snapshot of the pressure field at a given time $t=1.8s$ . It is produced by the spectral collocation model for case 5 . . . . .	27



# 1

## Introduction

---

A model designated BORIS (BOttom Response from Inhomogeneities and Surface) has been developed and implemented at SACLANTCEN [1, 2, 3]. The model has been compared with data recorded with a TOPAS PS-040 parametric sonar [2], demonstrating successfully the capabilities of the model to account for the main underwater acoustic scattering mechanisms. The model has also been used for inversion of seabed properties [4], and for examining the variability of the time-domain signal as a function of the source motion [5].

The purpose of this report is to compare the BORIS model with one based on the spectral collocation method developed at Forsvarets Forskningsinstitut (NDRE). As the models depend on different assumptions, a complete comparison is not possible, and a one-to-one relationship between the results can not be expected. However, the comparison of the results enables the study of effects from certain parameters which are difficult to study by comparison with data. In particular this is the case for the effects of interface roughness and volume inhomogeneities.

Five test were defined for the comparison of the results. The source, pulse and depth were unchanged to facilitate the comparison. The test cases were designed to emphasize and separate the effect of the interface roughness and volume inhomogeneities. The first test case consists of a flat, inhomogeneous bottom. The complexity of the bottom is then gradually increased to a rough, inhomogeneous bottom for the last test case.

# 2

## BORIS model

---

The model is designated BORIS which is an abbreviation for “BOttom Response from Inhomogeneities and Surface”. The theoretical basis of the model is described in [1], the verification and testing in [2], and the detailed specification of the implementation in [3].

The following integral [1] forms the basis of the model:

$$\begin{aligned} p(\mathbf{P}, t) &= p_s(\mathbf{P}, t) + p_v(\mathbf{P}, t) \\ &= \int_S dp_s(\mathbf{P}, t) + \int_V dp_v(\mathbf{P}, t) \end{aligned} \quad (1)$$

This integral expresses that the pressure field received at the source  $\mathbf{P}$  from the seafloor is the sum of the elementary pressure fields over the seafloor surface ( $S$ ) and the seafloor volume ( $V$ ). For a monostatic source and receiver with directivity pattern  $D_i$  and  $D_r$ , the seafloor surface contribution is given by

$$\begin{aligned} dp_s(\mathbf{P}, t) &= \frac{\cos(\gamma(\mathbf{R}))}{2\pi \bar{c}_0 R_0^2} p_0 \\ &\times (D_i D_r(\mathbf{R})) \mathfrak{R}_{01}(\mathbf{R}) e'(t - \frac{2R_0}{\bar{c}_0}) d\mathbf{S}_{\mathbf{R}} \end{aligned} \quad (2)$$

Here,  $\mathfrak{R}_{01}$  is the local water-sediment plane wave reflection coefficient at the point  $\mathbf{R}$ ,  $\bar{c}_0$  is the average sound speed in water,  $\gamma(\mathbf{R})$  is the angle between the incident direction and the vector  $\mathbf{n}$  normal to the surface at  $(\mathbf{R})$  and  $p_0$  is the source level.  $e'(t)$  is the time derivative of the transmitted pulse  $e(t)$ .

The volume contribution is given by

$$dp_v(\mathbf{P}, t) = \frac{-n_1^2(\mathbf{R}')}{2\pi R_0^2 \bar{c}_0^2} \mu(\mathbf{R}') p_0$$

$$\begin{aligned}
 & \times D_i(\mathbf{R}) D_r(\mathbf{R}) \mathfrak{S}_{01}(\mathbf{R}) \mathfrak{S}_{10}(\mathbf{R}) \\
 & \times \left( \frac{1}{\pi} \frac{\frac{\alpha R_1}{2\pi}}{(\frac{\alpha R_1}{2\pi})^2 + t^2} * e''(t - 2(\frac{\bar{n}_1 R_1 + R_0}{c_0})) \right) \\
 & \times d\mathbf{V}_{\mathbf{R}}
 \end{aligned} \tag{3}$$

In this expression,  $\bar{n}_1$  is the average refractive index in the first few metres of the bottom,  $n_1$  is the local refractive index at location  $\mathbf{R}'$  and  $R_1$  is the distance of penetration into the sediment.  $\alpha$  is the attenuation coefficient,  $\mathfrak{S}_{01}(\mathbf{R})$  and  $\mathfrak{S}_{10}(\mathbf{R})$  are the plane wave transmission coefficients. The double time derivative of the transmitted pulse  $e(t)$  is denoted by  $e''(t)$  and  $*$  denotes convolution.

These equations give the sound pressure level for a given time  $t$  at position  $\mathbf{P}$  by integration over the surface ( $S$ ) and the volume ( $V$ ). The local incident angle  $\gamma(\mathbf{R})$ , the local reflection coefficient  $\mathfrak{R}_{01}(\mathbf{R})$  and the local degree of inhomogeneities in the volume  $\mu(\mathbf{R}')$  are assumed to be known. Instead of using average quantities for these parameters, a different approach has been adapted. Before the calculations are carried out for the integral over  $S$ , one realization of the seafloor surface and volume is calculated based on a statistical set of parameters. The calculations are based on the Fourier synthesis method. For the surface, a filtered power law spectrum is used to calculate the height field, while for the volume part an exponential correlation function has been used to generate the inhomogeneity field. The model includes 3D rotation and position matrices for the source and receiver which allows for variations of position, heave, pitch and roll.

It is important to notice that the model has a stochastic nature, and that the result from one run to another will be different even with the same input parameters. This is because there is an infinite number of realizations of the seafloor for a fixed set of statistical parameters. However, the same realization might be used in several runs by controlling the random generator used in the model. A simplified block diagram of the model is shown in Fig. 1

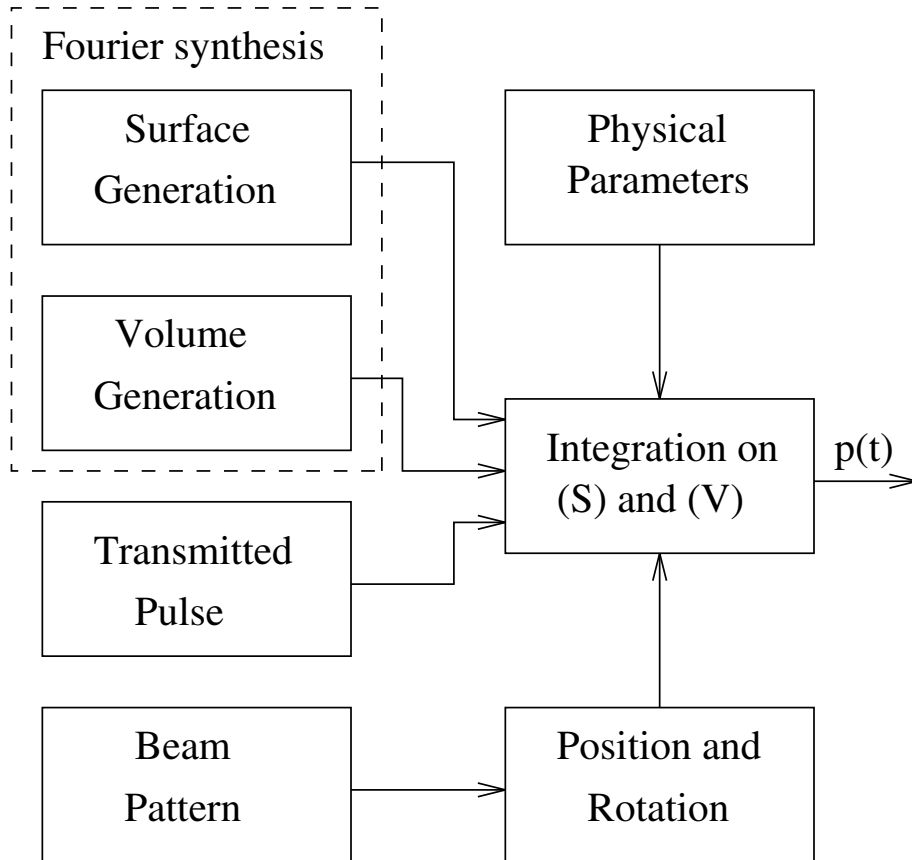


Figure 1 Simplified box diagram of the model.

## 3

Spectral collocation model

---

*3.1 Numerical methods for rough surface scattering problems*

Many methods exist for calculating the field scattered from rough surfaces [6]. The method of small perturbations is valid for a surface which is slightly rough and has small surface slope. The Kirchhoff approximation is valid for problems where the wavelengths are short relative to the roughness (radius of curvature) of the surface, but can be applied when the surface height is not negligible compared with the wavelength. Both these methods ignore the effects of multiple scattering at a rough surface. Methods are available, which sum contributions from distributions of surface irregularities to partially include multiple scattering.

Integral equation techniques [6] may be used to derive methods which require fewer limiting assumptions and are therefore more accurate than the approximations described above. However, the solution of integral equations generally requires the use of numerical methods.

Numerical methods, such as the finite difference or finite element [7] methods, have the potential of computing solutions to complex scattering problems with few limiting assumptions. A major limitation of these methods is that they are computationally intensive. The models are typically restricted by computational limitations to 2D problems with ranges of a few tens of wavelengths.

In this work the linearized acoustic equation is solved using the spectral collocation method [8]. The spectral collocation method requires generally fewer grid points per wavelength for numerical stability than finite differences, and the method has very low numerical dispersion and diffusion.

The model is a full-wave solution, i.e., it includes backscatter and all multiple interactions between scatters. Interface roughness and volume inhomogeneities with length scale of the order of the acoustic wavelength can be studied with the model.

For rectangular grids the discretization of the seafloor profile imposes a stair-step micro-roughness onto the larger scale topography. Dougherty [9] has shown that significant scattering can be caused by this micro-roughness. Hence the specification of complex seafloors may require a much finer grid than is necessary for numerical

stability and accuracy. This problem can be avoided by deforming the grid in order that the interface lies directly on a grid line. Such methods are described by Fornberg [10] and Lie [11].

### 3.2 *Physical model and numerical implementation*

The problem we will study is the scattering of a beam at a rough bottom with volume inhomogeneities. Figure 2 illustrates the model configuration.

An acoustic source (array) is located in an homogeneous water column above a rough, inhomogeneous bottom. The height of the source over the bottom is such that the interaction of the beam with the bottom occurs in the far-field of the source.

Although only monostatic scattering will be considered, bistatic scattering is easily achieved with the present model as illustrated in the figure.

With the requirement that the interaction of the beam with the bottom occurs in the far-field of the source, a grid or computational domain containing the source and receiver will be far too large. Instead, a small computational domain containing the rough, inhomogeneous bottom with only a very shallow water layer is used. The source signal is computed analytically and introduced along the top of the computational domain at each time step. For propagating the scattered signal from the top of the computational domain back to the receiver, the Kirchhoff-Helmholtz formulation is used. The method requires the water column above the rough bottom to be homogeneous, and that outgoing energy from the computational domain propagates out of the domain without reflections at the boundaries.

The spectral collocation method [8] is used to solve the linear acoustic equations inside the computational domain. The equations are solved in Cartesian coordinates. Depth- and range-dependent sound speed and density, and variations in bottom topography are implemented by specifying the appropriate values at the gridpoints. The conditions at the upper and lower boundaries are constructed to give free transmission of waves through the boundaries.

The model is a time-domain model. A smooth, symmetric pressure pulse is used for the source. A beam is generated by using a source array with elements spaced approximately  $\lambda/2$ . The output of the model is 'snapshots' of the pressure- and velocity-fields at selected times, and time series at selected gridpoints.

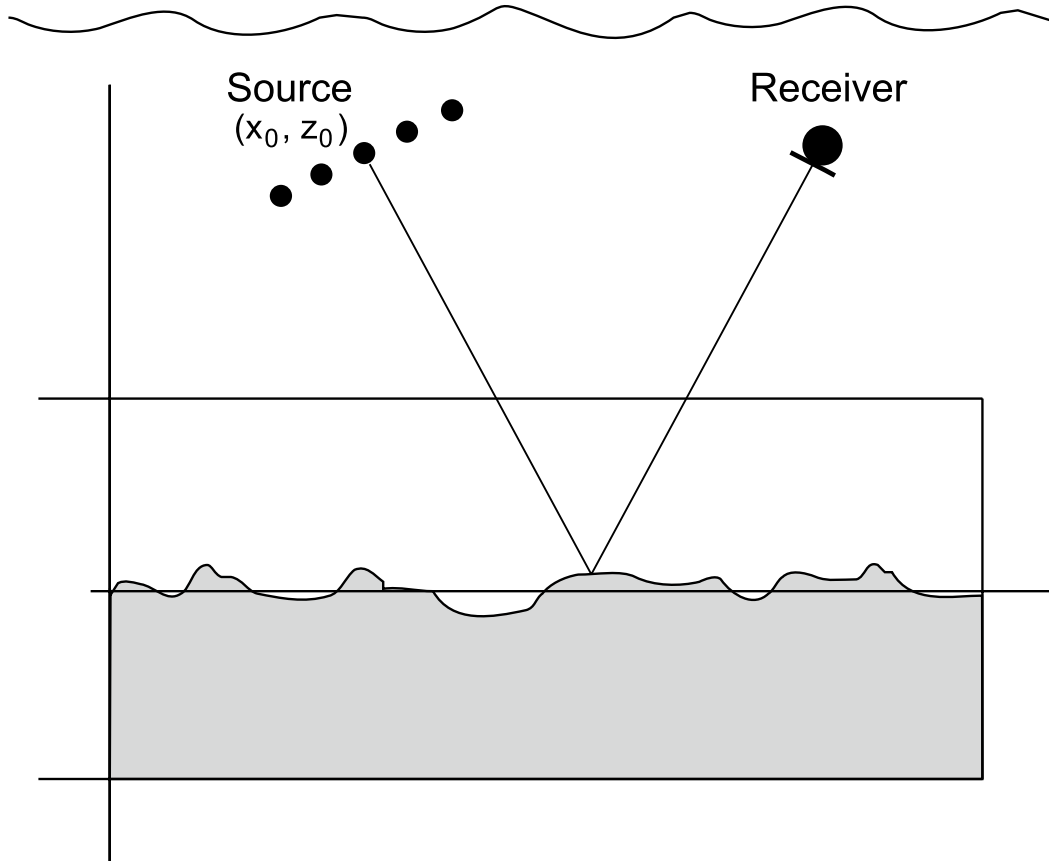


**Figure 2** Model geometry for the scattering problem. The computational grid is rectangular with dimensions  $L_x=7.68$  m,  $L_z=1.98$  m in  $x$  and  $z$ -direction respectively. A beam is generated by the source array of 21 elements located at  $x_0=3.84$  m,  $y_0=9.6$  m above the computational grid. The source generates a short pressure pulse centered at 6.0 kHz. For monostatic scattering a single receiver is located at the centre of the array  $(x_0, y_0)$ .

### 3.2.1 The Basic Equations

The equations used to model the wave motion are the linearized acoustic equations. Consider two-dimensional motion in Cartesian coordinates  $(x, z)$  where  $x$  is the horizontal axis and  $z$  is the vertical axis. By writing the components of the velocity vector as  $\mathbf{v} = (u, w)$ , the components of the fluid equations become

$$u_t = -\frac{1}{\rho_0} p_x \quad (4)$$

$$w_t = -\frac{1}{\rho_0} p_z \quad (5)$$

$$p_t = -\rho_0 C^2 (u_x + w_z) \quad (6)$$

Here  $(u, w, p)$  are perturbation quantities and  $\rho_0(x, z), C(x, z)$  are density and sound velocity respectively.

The equations of fluid motion are given in physical units. For numerical computations it is convenient to transform the equations into non-dimensional form. Non-dimensional variables (unmarked) are introduced by normalizing the physical variables (indicated by an asterisk) as follows:

$$\rho = \frac{\rho^*}{\rho_0^*}, \quad u = \frac{u^*}{V_0^*}, \quad w = \frac{w^*}{V_0^*}, \quad p = \frac{p^*}{\rho_0^* (V_0^*)^2}, \quad (7)$$

$$x = \frac{x^*}{L_0^*}, \quad z = \frac{z^*}{L_0^*}, \quad t = \frac{V_0^*}{L_0^*} t \quad (8)$$

With these choices the normalized speed of sound becomes  $C = C^*/V_0^*$  and the equations remain of the same form in the non-dimensional quantities.  $\rho_0^*, V_0^*$  are chosen to be the density and sound velocity at the source, while  $L_0^*$  is the water depth.

### 3.2.2 The Numerical Scheme

Equations 4 - 6 are solved using a spectral collocation method described by Canuto *et al.* [8]. A semi-discretization method is used, where the spatial term is discretized first, reducing the partial differential equation to a system of ordinary differential equations. An attractive feature of semi-discretization is that several techniques are available [12] to solve the semi-discrete form of the original partial differential equations. The time integration scheme used here is an explicit second-order Runge-Kutta method.

The spatial discretization is spectral, i.e. the solution is represented by infinitely differentiable global functions (as opposed to finite difference schemes which use local functions). Trigonometric functions and Chebychev polynomials are used to describe the horizontal and vertical structure, respectively. As a result, the solutions are periodic in the horizontal direction and admit aperiodic solutions in the vertical direction. The error in the discretization of a smooth interface not aligned with the grid acts as a source of unphysical noise unless the interface has roughness on this scale. This source could have been eliminated by using interface mapping.

The problem can be formulated as

$$U_t + A_1 U_x + A_2 U_z = f \quad (9)$$

where  $U = [u, w, p]^T$ . The spectral method approximates the solution  $U$  by a finite series

$$\hat{U}(x, z, t) = \sum_{n=0}^{N_x-1} \sum_{m=0}^{N_z} a_{mn}(t) e^{imx} T_n(z), \quad (10)$$

where  $T_n$  is the Chebychev polynomial of order  $n$ , and  $a_{mn}$  are complex coefficients. The domain of definition of the basis functions is  $[0, 2\pi] \times [-1, 1]$ . This choice of basis functions leads to a set of collocation points (the grid) given by

$$x_m = 2\pi m/N_x, \quad 0 \leq m \leq N_x - 1 \quad (11)$$

$$z_n = \cos(2\pi n/N_z), \quad 0 \leq n \leq N_z \quad (12)$$

The spectral collocation solution to the equations gives the requirements that the approximate solution should satisfy the equations at the collocation points:

$$\frac{d}{dt} \hat{U}(x_m, z_n, t) + A_1 \hat{U}_x(x_m, z_n, t) + A_2 \hat{U}_z(x_m, z_n, t) = f_1(x_m, z_n, t) \quad (13)$$

This is a set of ordinary differential equations in time. The set of equations is integrated in time by an explicit second-order adaptive Runge-Kutta method.

At the upper and lower boundaries, open boundary conditions are implemented using a method suggested by Gustafsson [13]. The boundary conditions are formulated on differential form [14], i.e. given as differential equations, which are integrated together with the equations for the interior points. Periodic boundary conditions are used for the sides, where the numerical grid corresponds to the sides of the box in Fig. 2.

# 4

## Differences between the models

---

As the two models are based on two totally different approaches, an unambiguous one-to-one comparison is not possible. In this section, the main differences and their implications are discussed.

### 4.1 *Two versus three dimensions*

The main limitation in the comparison between the two models lies in the fact that the spectral collocation model is two dimensional, whereas the BORIS model uses a three dimensional approach. Even though the spectral collocation model could have been implemented in 3D, the run-time and storage allocation of the model are currently too high for practical use. The BORIS model can be run in a 2D mode, but the way the equations are implemented would require a spatial resolution which will be too high for the spectral collocation model.

The approach used in this report is to run the BORIS model in 3D which generates a 3D surface and volume. A 2D slice of this surface and volume is then used as input to the spectral collocation model. With this approach the two models can be run without major modifications, but the limitations introduced must be taken into consideration. The total scattering from the surface and volume consists of a sum of coherently added contributions. If the contributions are totally random with a zero mean, the sum would be zero. In reality the contributions are not randomly distributed, but the contributions from the 3D model will introduce more randomness in the contributions than the 2D model. Therefore, the 3D model is expected to have a lower amplitude on the backscattered pressure field than the 2D model in the presence of a rough surface or volume inhomogeneities.

An alternative would have been to run the spectral collocation model in a N\*2D approach. That is, the 2D model is run on a number of 2D slices through the 3D seafloor and volume generated by BORIS, and the contributions from each slice are summed coherently to obtain the total scattered signal. This approach is better than the approach used, but as the spectral collocation model has a considerable run time, this approach could not be adopted for this report due to time constraints.

#### 4.2 *Single versus multiple scattering*

The BORIS model calculates the single return from each surface and volume element by integration over the insonified area. Any effect due to multiple scattering from the surface or in the volume will therefore be ignored.

The time domain spectral collocation method solves the two-way linear acoustic and elastic wave equation. Time domain solutions to the two-way wave equations contain all multiple interactions between scatters, including mode conversions between compressional, shear and interface waves. Interface roughness and volume inhomogeneities with length scale of the order of the acoustic wavelength can be studied with the model.

The effect of single *versus* multiple scattering on the time-series result is difficult to predict, as multiple scattering can both increase and decrease the total pressure depending on the phase coherence.

#### 4.3 *Inhomogeneity description*

In the BORIS model, the sediment inhomogeneity is described by the equation:

$$\mu(\mathbf{R}') = \gamma_c(\mathbf{R}') + \gamma_\rho(\mathbf{R}') \quad (14)$$

where  $\gamma_c$  and  $\gamma_\rho$  are respectively the relative fluctuation of the sound speed and of the density at the same location. These fluctuations are calculated as the variation around the mean values  $\bar{c}_1$  and  $\bar{\rho}_1$  in the total insonified volume:

$$\gamma_c(\mathbf{R}') = \frac{c_1(\mathbf{R}') - \bar{c}_1}{\bar{c}_1} \quad (15)$$

$$\gamma_\rho(\mathbf{R}') = \frac{\rho_1(\mathbf{R}') - \bar{\rho}_1}{\bar{\rho}_1} \quad (16)$$

For the spectral collocation model the separate variation of the sound speed and the density is needed, whereas only the sum  $\mu(\mathbf{R}')$  is available from the BORIS model. According to core analysis done by Hamilton [15] and Yamamoto [16], these two variables are independent. For the comparison between the models, the two variables are treated as proportional such that

$$\gamma_\rho(\mathbf{R}') = K \gamma_c(\mathbf{R}') \quad (17)$$

where  $K$  is the proportionality factor. The local sediment sound speed and density used by the spectral collocation model are then given by

$$c_1(\mathbf{R}') = \bar{c}_1 \left( 1 + \frac{1}{K+1} \mu(\mathbf{R}') \right) \quad (18)$$

$$\rho_1(\mathbf{R}') = \bar{\rho}_1 \left( 1 + \frac{K}{K+1} \mu(\mathbf{R}') \right) \quad (19)$$

#### 4.4 Attenuation

Attenuation is not implemented in the spectral collocation model. For the comparison, attenuation is therefore set to zero in the BORIS model in order not to introduce any difference in the results due to attenuation.

#### 4.5 Bottom discretization

The BORIS model generates a bottom which is used as input to the spectral collocation model as described above. The spectral collocation model uses a grid that is equidistant in  $x$ -direction, but in  $z$ -direction the non-equidistant Gauss-Lobatto points are used:

$$(x_i, z_j) \mid x_i = i/N_x, z_j = \cos(\pi j/N_z), \quad (20)$$

$$i = 0, \dots, N_x - 1, j = 0, \dots, N_z$$

where the number of points in the  $x$  and  $z$  direction are  $N_x$  and  $N_z$ . Input data from BORIS are equidistant in both  $x$  and  $z$ -direction, and an interpolation is therefore carried out in order to generate the grid used by the spectral collocation model. The resulting resolution is the same in both models.

## 5

## Simulation setup

## 5.1 Pulse and geometry

The pulse, beam pattern and geometry are selected in order that both models can operate within their limits. An area of  $7.68 \times 7.68 \text{ m}^2$  is insonified by a source located 9.6 m over the bottom at normal incidence. The source generates a pressure pulse

$$p(t) = \sin(\omega t) - \frac{1}{2}\sin(2\omega t), \quad 0 \leq t \leq 2\pi/\omega \quad (21)$$

centered at 6.0 kHz. The source is a linear array (planar in the case of 3D) of 21 point sources with an element spacing of  $\lambda/2 = 0.125 \text{ m}$ . The array is amplitude weighted in order to decrease the sidelobes in the beam pattern. The pressure pulse and the resulting beam pattern measured 9.6 m away from the source are shown in Fig. 3 and Fig. 4 respectively. The maximum bottom penetration taken into account is 1 m. The resolution of both the seafloor surface and the volume is 1.5 cm. The sampling frequency used for the BORIS model was 520 kHz, which corresponds to the step size, or sampling interval, used by the spectral model. The sampling interval is determined by stability conditions, and is much smaller than that which is required to represent the pulse.

The BORIS parameters used for the runs are shown in Table 1, while Table 2 shows the parameters used for the spectral collocation model. It should be noted that the same statistical realization of the seafloor and volume were used in order to compare the different test cases.

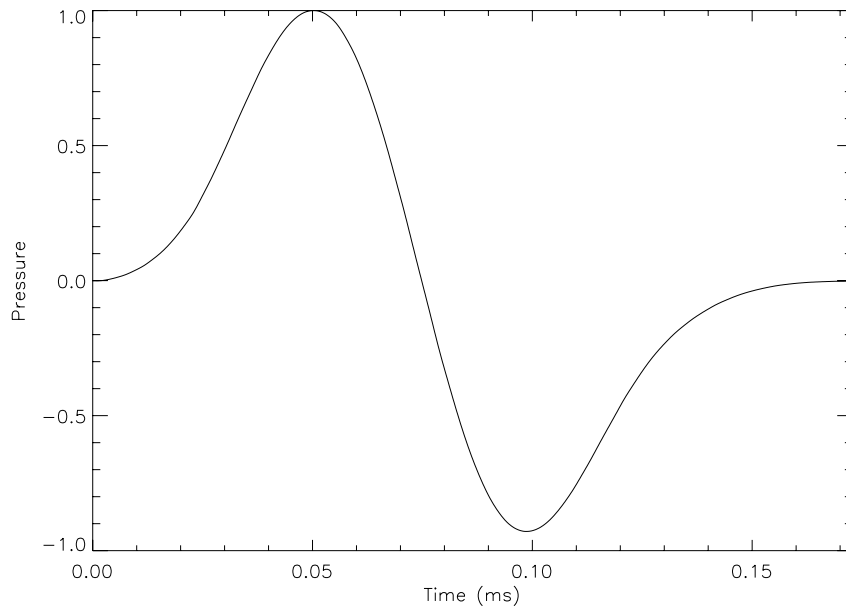


**Figure 3** *The time-series of the pulse*

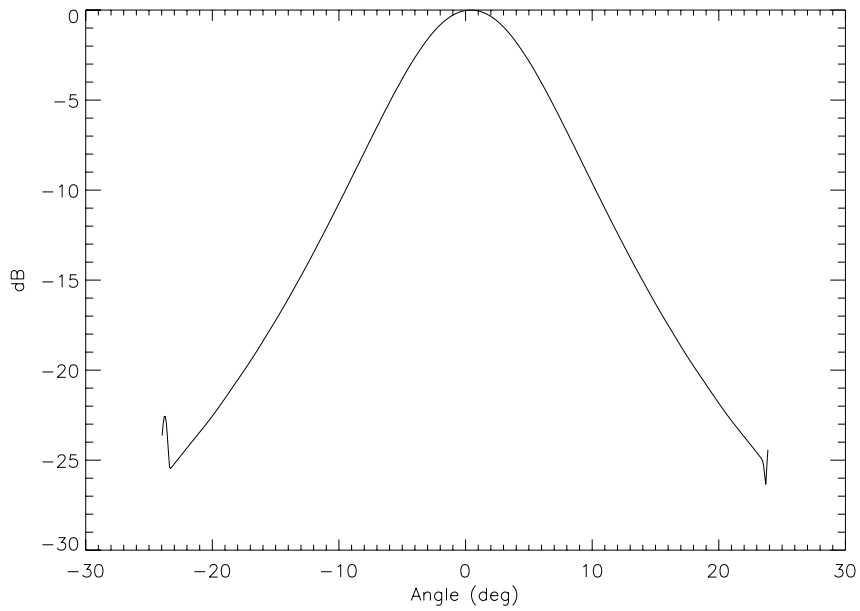


**Figure 4** *The beam pattern of the source*

**Table 1** *BORIS model parameters.*

Parameters	Symbol (Unit)	Value
Surface resolution	$dp_s$ (m)	0.015
Surface length	- (m)	7.68
Volume resolution	$dp_v$ (m)	0.015
Source depth	$H$ (m)	9.6
Sediment sound speed	$c_1$ (m/s)	1720
Sediment density	$\rho_1$ ( $g/cm^3$ )	1.90
Surface rms roughness	$\sigma_h$ (m)	0.03
Surface power exponent	$\nu$	2.0
LP cutoff	$K_{lp}$ (rad/m)	30
HP cutoff	$K_{hp}$ (rad/m)	1
Volume rms inhomogeneity	$\mu$	0.05
Volume depth	- (m)	1.0
Volume Horizontal Correlation	$l_h$ (m)	0.5
Volume Vertical Correlation	$l_v$ (m)	0.02
Attenuation	$\beta$ (dB/m)	0.0

**Table 2** *Spectral collocation model parameters.*

Parameters	Symbol (Unit)	Value
Model		a7e
Grid in x,z direction		Fourier x Chebychev
Gridpoints in x-direction	NX	512
Gridpoints in z-direction	NZ	128
Scaling in x-direction	scale_x	4.0
Scaling in z-direction	scale_z	1.0
Scaling of length	L0 (m)	0.96 m
Dimension of computational domain	$L_x$ (m), $L_z$ (m)	7.68, 1.92
Scaling of velocity	V0 (m/s)	1500
Scaling of density	$\rho_0$ ( $kg/m^3$ )	1000
Source frequency	$f_c$ (Hz)	6000
Source location	x0,y0 (non-dim)	pi,10
Elements in source array		21
Element distance		$\lambda/2$
Source array weighting		Welch
Time series recorded at interval	(nondim)	0.003
Source type		Spherical
Model time	(non-dim)	0.0 - 3.0

# 6

## Model comparison results

---

This section presents the results from the five comparisons carried out between the two models. The figures produced can be found in Annex A. The bottom characteristics of the five test cases can be seen by looking at the two dimensional sound velocity profile, Fig. 5 - 9. For case 1, the bottom is flat and homogeneous, and the sound velocity profile (Fig. 5) is a simple step function. Case 2 has a rough surface and homogeneous volume. In case 3, the main impedance of the volume is the same as that of water, but variations around the mean values make the volume inhomogeneous. The surface is flat. Figure 8 shows the resulting sound velocity profile for case 4. The volume is inhomogeneous, and there is an impedance contrast between the flat bottom and the water. Finally, case 6 includes both the volume inhomogeneities, impedance contrast and rough surface.

### 6.1 Case 1: Flat and homogeneous bottom

This case is the simplest one where the bottom is flat (no roughness) and the volume is homogeneous. For this special case the 2D/3D problem is not present because the bottom is equal in all directions. The 2D propagation is properly taken into account in the spectral collocation model. Figure 10 shows the results from the BORIS simulation. The small peak at the right is due to the truncation of the beam at  $25^\circ$  and is artificial. Figure 11 shows the result from the spectral collocation model corresponding to the spatial position of the BORIS source. As with the BORIS model, an artificial return occurs at  $t=0.014$  s, due to the finite horizontal integration range of the Kirchhoff-Helmholtz integral. If the model domain is made larger in the horizontal direction, the artificial pulse will appear later, hence leaving a longer portion of the scattered signal unaffected. For the spectral collocation model, some noise can also be seen just after the main reflection. This artifact is due to reflections from the left and right boundaries of the model but can be reduced or removed by making the model domain larger in the horizontal direction, or by using a narrower beam. Some numerical noise can be seen just after the main reflection, but compared to the amplitude of the pulse this can be disregarded. However, for both models the artificial return to the right will be present also in the following cases, and therefore the signal is truncated earlier in the following cases.

The shapes of the two signals are similar, but not identical. Both models show

that the negative peak has a slightly higher amplitude than the positive peak. For the transmitted pulse the situation is the opposite. The fact that the pulse is not a perfect reflection of the transmitted pulse is correct as the source is not a point source [2]. The reason for the small difference in the pulse shape between the two models for this special case is probably due to a non-valid approximation in the BORIS model. The model assumes that the pulse shape is unchanged over the whole beam, but as seen from Fig. 14 the pulse changes shape depending on the position in the beam.

### 6.2 Case 2: Rough and homogeneous bottom

For this case a roughness with an rms value of 4 cm is introduced in the seafloor surface (see Tab. 1 for other parameters). All the other parameters are kept equal to the setting in case 1. The roughness can be seen in Fig. 6 where the resulting sound velocity profile is shown. The effect of the roughness is to spread the energy out in time, thereby reducing the maximum amplitude of the signal and introducing a tail behind the coherent part of the reflection. The results from the BORIS models are shown in the lower plot in Fig. 12. The result from the spectral collocation model is shown in the lower plot in Fig. 13. The result from the BORIS model has a lower amplitude of the coherent reflection and more random behavior than the result from the spectral collocation model. The difference is probably due to the 2D/3D problem and the difference corresponds to the expected behavior as described in section 4.1. Even though there are differences in the signals, the overall characteristics and amplitude of the signals are similar<sup>1</sup>.

### 6.3 Case 3: Flat and inhomogeneous bottom without impedance contrast

In this case we look at the volume contribution only. This is obtained by setting the impedance contrast equal to zero, i.e. the average sound speed and density of the bottom equals the corresponding values for the water column. The result is an introduction of a sound speed and density fluctuation at the seafloor interface as seen in Fig. 7. The horizontal periodicity in the fluctuations is due to the way the BORIS model implements the volume inhomogeneities. From Figs. 12 and 13 the results from the two models can be studied. Again, the signal from the BORIS model has a lower amplitude and more random behavior as expected. It is encouraging to see that the volume contributions from both models are in the same order of magnitude with respect to amplitude.

---

<sup>1</sup>The difference of approximately  $25\mu s$  in the arrival time between the two signals is due to a discretization error and should be ignored.

#### 6.4 *Case 4: Flat and inhomogeneous bottom*

This case consists of a combination of case 1 and case 3 with a flat surface but an inhomogeneous bottom (Fig. 8). The results from both models illustrate that the time-series produced look similar to the coherent sum of the result from case 1 and case 3. This might be explained by Eq. (1) which states that the total scattering from the seafloor can be treated as the coherent sum of the volume and surface scatter. It is important to note that the impedance contrast will change both the shape and the amplitude of the volume part compared to the volume contribution in test case 3. Therefore the coherent sum of case 1 and case 3 will look similar to, but not be identical to the results for case 4.

#### 6.5 *Case 5: Rough and inhomogeneous bottom*

This case may be viewed as the combination of case 2 and case 3. The seafloor surface is rough, and the volume is inhomogeneous (Fig. 9). The results follow the same trends as described in the previous cases. A snapshot of the pressure field from the spectral collocation model is also shown in order to illustrate the spatial properties of the field. The field is plotted just before the backscattered pulse reaches the upper boundary of the model.

## 7

Summary

---

In this report, results from the BORIS model have been compared with results from a model based on the spectral collocation method. The purpose of the comparison has been to increase the confidence in the model results and to understand the implications of the assumptions and limitations built into the models. The comparisons show that the two models produce comparable results from all test cases. The comparisons suffer from the fact that the BORIS model is a 3D model whereas the spectral collocation model is 2D. One of the implications of that is that the spectral collocation model predicts a slightly higher amplitude on the backscattered signal than the BORIS model. Also, a one-to-one match in the shape of the signals from the volume and the surface can not be expected. Given the limitations in the comparison itself, the result are considered to be encouraging for both models. The general and expected trends are followed by both models, and the levels of the scattering due to surface roughness and volume inhomogeneities are comparable.

### 7.1 *Future work*

In order to overcome the 2D versus 3D problem, future work will concentrate on running the spectral collocation model over several 2D slices through the 3D seafloor and volume generated by BORIS. This way the contributions from each slice can be summed coherently to obtain a prediction of the full 3D scattered signal. An improved model setup will also use a computational domain that is larger in the horizontal direction for the spectral collocation model. This will shift the artificial returns caused by the finite horizontal range to a later time, leaving a longer portion of the scattered signal uncorrupted.

## References

---

- [1] Pouliquen, E., Bergem, O., Pace, N.G. Time-evolution modelling of seafloor scatter, Part1: Theory. SACLANTCEN SM-328, NATO UNCLASSIFIED. La Spezia, Italy, NATO SACLANT Undersea Research Centre, 1997
- [2] Bergem, O., Pouliquen, E., Canepa, G., Pace, N.G. Time-evolution modelling of seafloor scatter, Part2: Experimental verification. SACLANTCEN SM-327, NATO UNCLASSIFIED. La Spezia, Italy, NATO SACLANT Undersea Research Centre, 1997
- [3] Canepa, G., Bergem, O., Pouliquen, E. The implementation of BORIS-3D: Bottom Response from Inhomogeneities and Surface, Version 1.0. SACLANTCEN M-125, NATO UNCLASSIFIED. La Spezia, Italy, NATO SACLANT Undersea Research Centre, 1997
- [4] Caiti, A., Bergem, O., Pouliquen, E., Biancheri, A., Scaricaciottoli, S. Seabed Characterization by Inversion of Parametric Sonar Data: Selection of the Cost Function. *In* Pace, N.G., Pouliquen, E., Bergem, O., Lyons, A., *editors*. High Frequency Acoustics in Shallow Water. La Spezia, Italy, NATO SACLANT Undersea Research Centre, 1997. pp. 83-90. [ISBN 88-900194-1-7]
- [5] Bergem, O., Pouliquen, E., Pace, N.G. The effect of source movements on shallow water bottom backscatter. *In* Pace, N.G., Pouliquen, E., Bergem, O., Lyons, A., *editors*. High Frequency Acoustics in Shallow Water. La Spezia, Italy, NATO SACLANT Undersea Research Centre, 1997. pp. 25-30. [ISBN 88-900194-1-7]
- [6] Ogilvy, J.A. Theory of Wave Scattering from Random Rough Surfaces. Bristol Adam Hilger, 1991
- [7] Murphy, J.E. and Chin-Bing, S.A. A finite-element model for ocean acoustic propagation and scattering. *Journal of the Acoustical Society of America*, 86, 1989:1478-1483
- [8] Canuto, C., Hussaini, M.Y., Quarteroni, A. and Zang, T.A. New York, Springer, 1988
- [9] Dougherty, M.E. and Stephen, R.A. Seismo-acoustic propagation through rough seafloors. *Journal of the Acoustical Society of America*, 90, 1991:2637-2651
- [10] Fornberg, B. The pseudospectral method: Accurate representation of interfaces in elastic wave calculations. *Geophysics*, 53, 1988:625-637

- [11] Lie, I. Ocean-bottom interaction model in 3D. FFI/RAPPORT-94/04100, 1994
- [12] Hall, G. and Watt, J.M. Modern Numerical Methods for Ordinary Differential Equations. Oxford Univers. Press, 1976.
- [13] Gustafsson, B. Far-field boundary conditions for time dependent hyperbolic systems. Manuscript CLaSSiC-87-16, Stanford University, Stanford, (CA) 1987.
- [14] Bjørhus, M. The ODE formulation of hyperbolic PDE's discretized by the spectral collocation method. *SIAM Journal of scientific Computing*, 16, 1995:542-557
- [15] Hamilton, E.L. and Bachman, R.T. Sound velocity and related properties of marine sediments. *Journal of the Acoustical Society of America*, 72, 1982:1891-1903
- [16] Yamamoto, T. Acoustic scattering in the ocean from velocity and density fluctuation in the sediments. *Journal of the Acoustical Society of America*, 99, 1996:866-879

Annex A

Figures from test runs

---

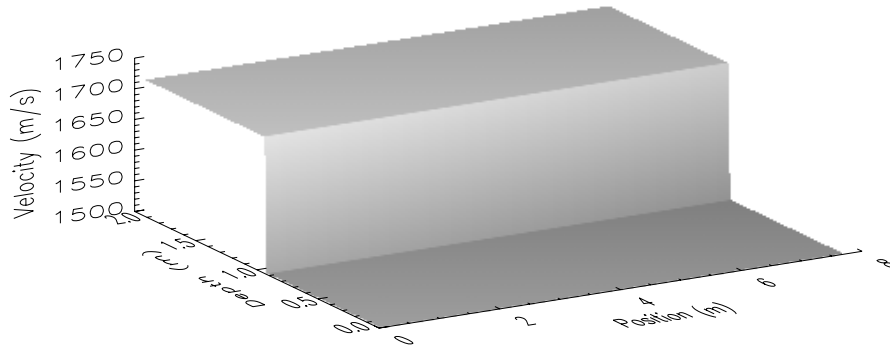


Figure 5 *The sound velocity profile, case 1*

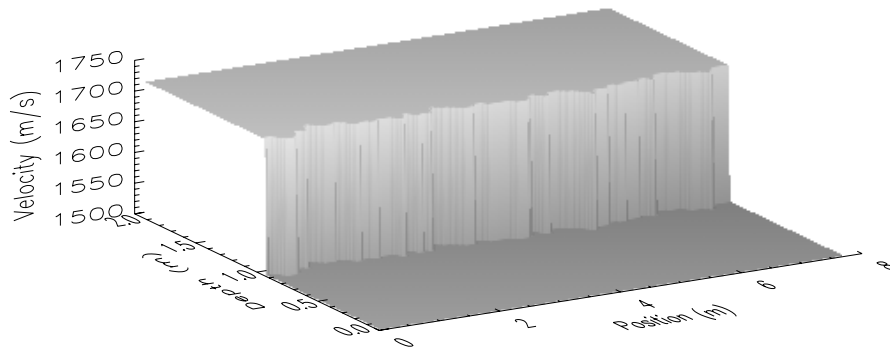


Figure 6 *The sound velocity profile, case 2*

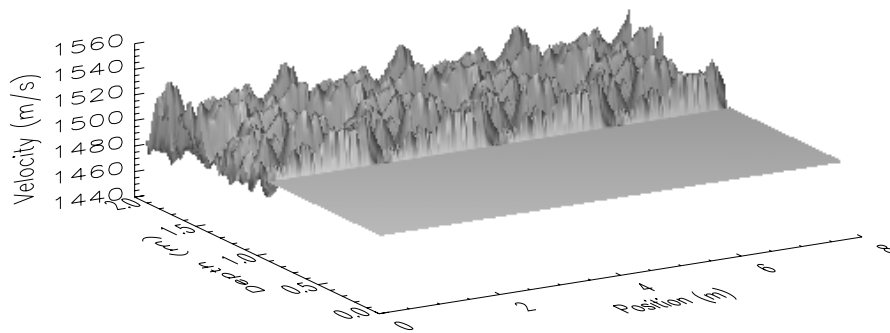


Figure 7 *The sound velocity profile, case 3*

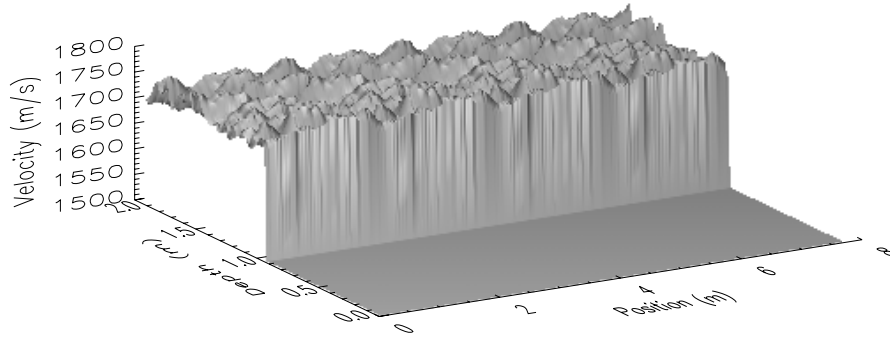


Figure 8 *The sound velocity profile, case 4*

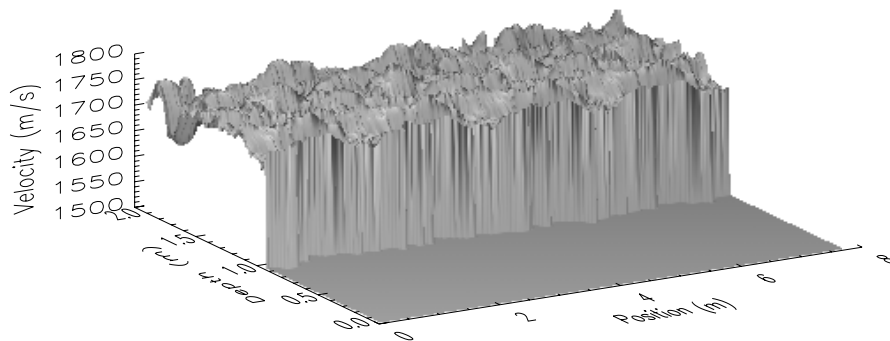


Figure 9 *The sound velocity profile, case 5*

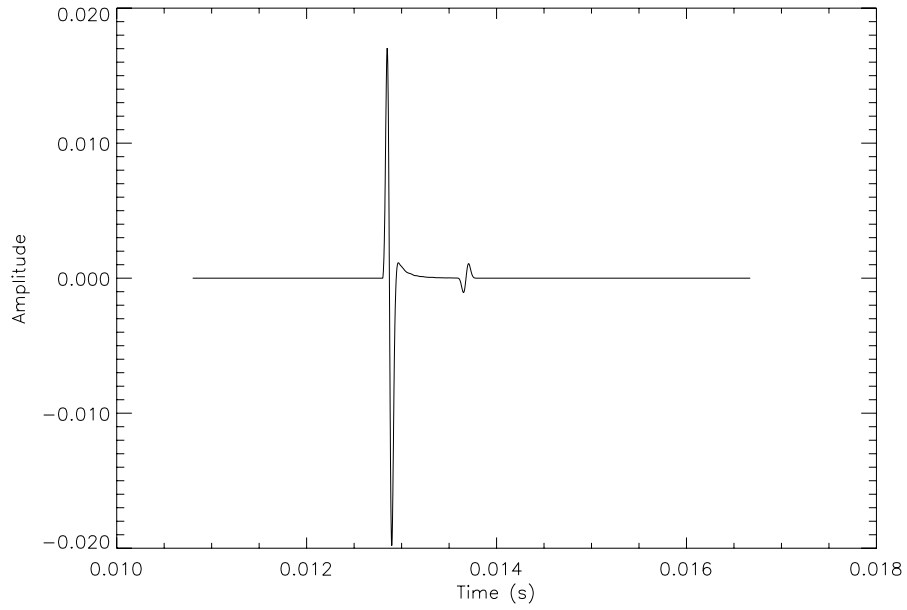


Figure 10 Result from BORIS, case 1

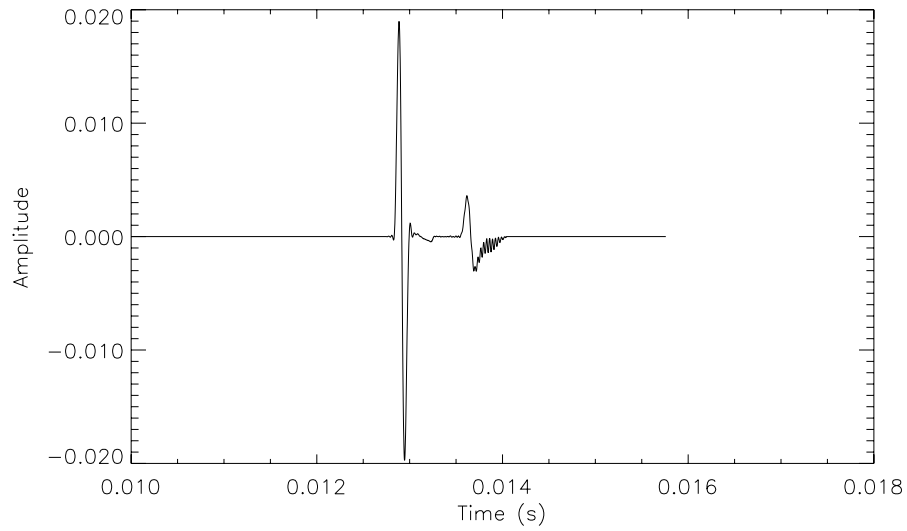


Figure 11 Result from spectral collocation model, case 1

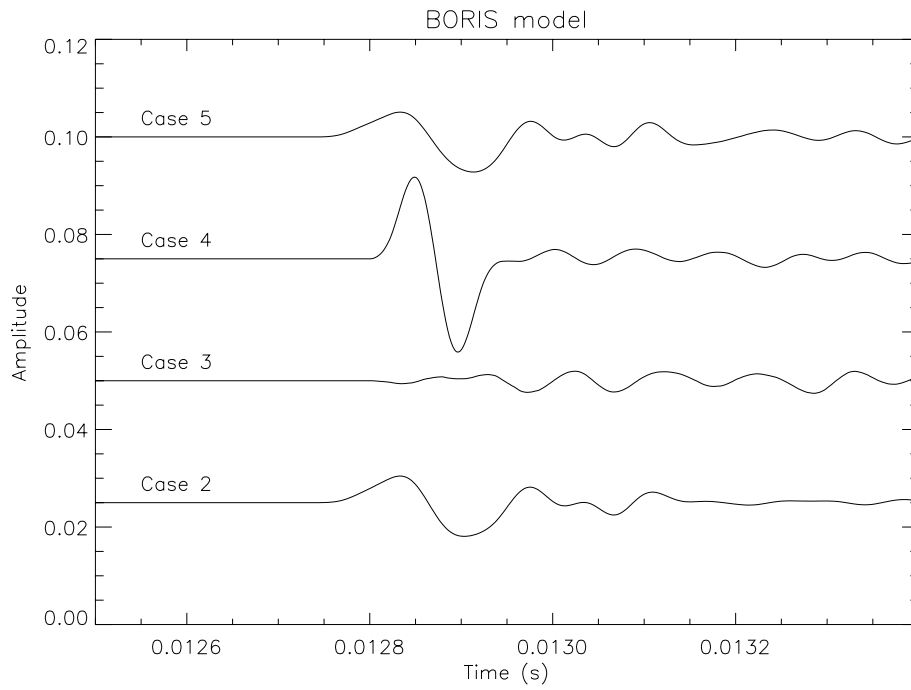


Figure 12 Result from BORIS, case 2-5

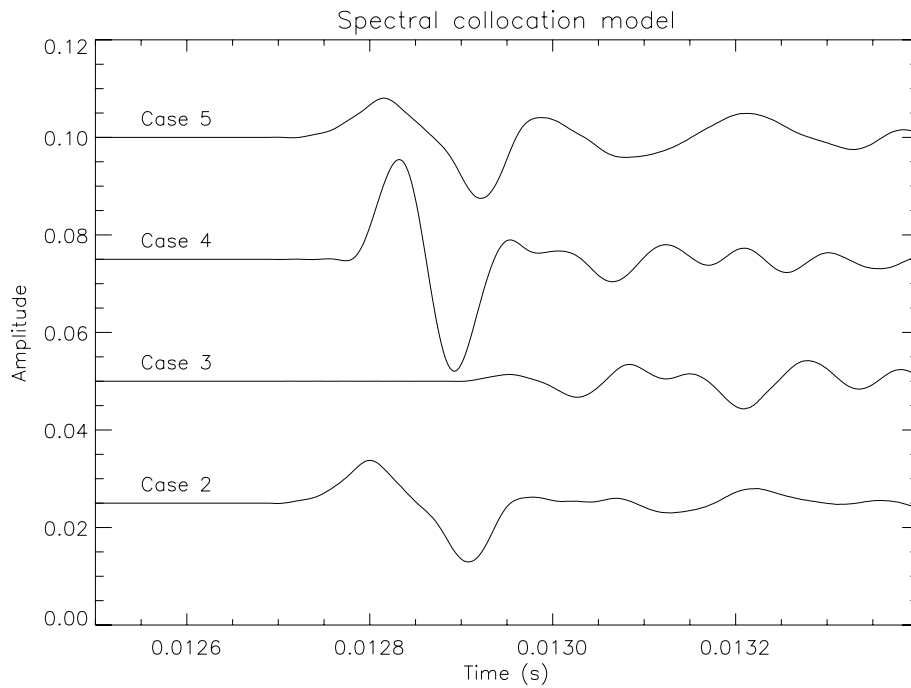
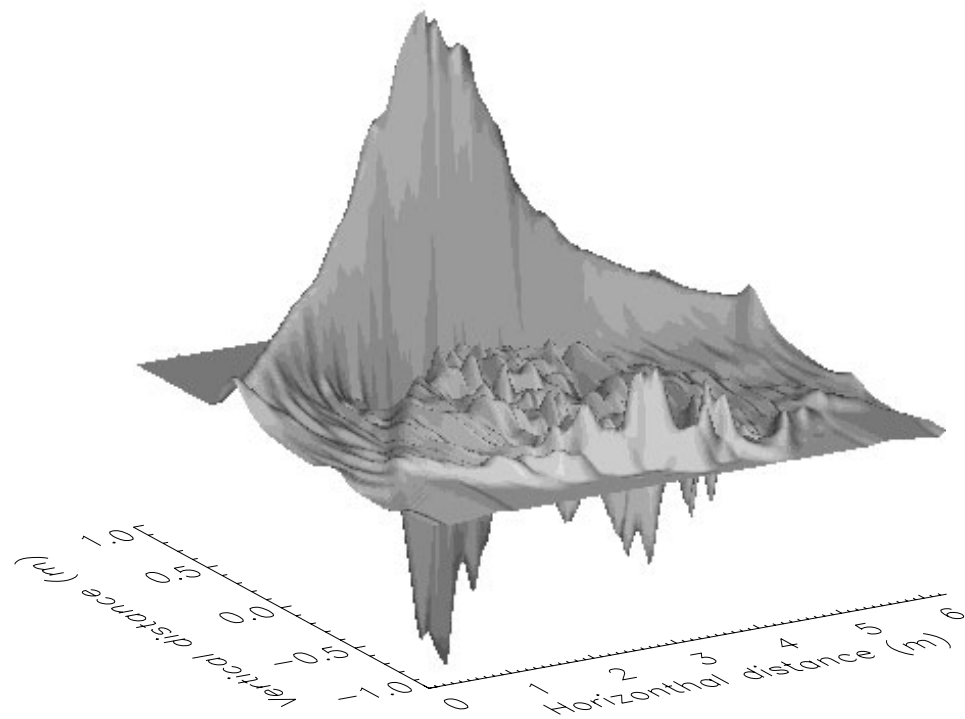


Figure 13 Result from spectral collocation model, case 2-5



**Figure 14** The figure show a snapshot of the pressure field at a given time  $t=1.8s$ . It is produced by the spectral collocation model for case 5



NATO Undersea Research Centre  
Viale San Bartolomeo 400  
19138 La Spezia, Italy